AD-A237 672

AFGL-TR-87-0331

SSS-IR-88-9216
W/O 11304

Current Collection by a High-Voltage
Sphere from a Cold Magnetoplasma

M. J. Mandell
M. Rotenberg
I. Katz

S-CUBED
A Division of Maxwell Laboratories, Inc.
P. O. Box 1620
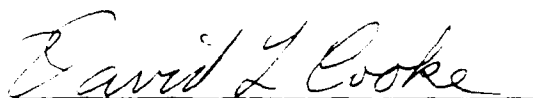La Jolla, CA 92038-1620

December 1987

Scientific Report No. 6

AIR FORCE GEOPHYSICS LABORATORY
AIR FORCE SYSTEMS COMMAND
UNITED STATES AIR FORCE
HANSCOM AIR FORCE BASE
MASSACHUSETTS 01731-5000

91-03939

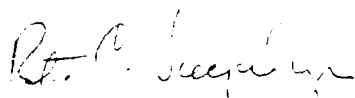" This technical report has been reviewed and is approved for publication "

DAVID L. COOKE
Contract Manager

CHARLES P. PIKE
Branch Chief

FOR THE COMMANDER

RITA C. SAGALYN
Division Director

REPORT DOCUMENTATION PAGE

Form Approved
OMB No. 0704-0188

1a. REPORT SECURITY CLASSIFICATION Unclassified			1b. RESTRICTIVE MARKINGS			
2a. SECURITY CLASSIFICATION AUTHORITY N/A			3. DISTRIBUTION/AVAILABILITY OF REPORT Approved for public release; distribution unlimited			
2b. DECLASSIFICATION/DOWNGRADING SCHEDULE N/A						
4. PERFORMING ORGANIZATION REPORT NUMBER(S) SSS-IR-88-9216			5. MONITORING ORGANIZATION REPORT NUMBER(S) AFGL-TR-87-0331			
6a. NAME OF PERFORMING ORGANIZATION S-CUBED Division Maxwell Laboratories, Inc.		6b. OFFICE SYMBOL (If applicable)	7a. NAME OF MONITORING ORGANIZATION Air Force Geophysics Laboratory			
6c. ADDRESS (City, State, and ZIP Code) P. O. Box 1620 La Jolla, CA 92038-1620			7b. ADDRESS (City, State, and ZIP Code) Hanscom Air Force Base MA 01731-5000			
8a. NAME OF FUNDING/SPONSORING ORGANIZATION Air Force Geophysics Laboratory		8b. OFFICE SYMBOL (If applicable)	9. PROCUREMENT INSTRUMENT IDENTIFICATION NUMBER F19628-86-C-0056			
8c. ADDRESS (City, State, and ZIP Code) Hanscom Air Force Base MA 01731			10. SOURCE OF FUNDING NUMBERS			

10. SOURCE OF FUNDING NUMBERS			
PROGRAM ELEMENT NO.	PROJECT NO	TASK NO.	WORK UNIT ACCESSION NO
62101F	7601	30	AA

11. TITLE (Include Security Classification)

Current Collection by a High-Voltage Sphere from a Cold Magnetoplasma

12. PERSONAL AUTHOR(S)
M. J. Mandell, M. Rotenberg, Ira Katz

13a. TYPE OF REPORT Technical report no. 6	13b. TIME COVERED FROM 2/87 TO 12/87	14. DATE OF REPORT (Year, Month, Day) 1987 December	15. PAGE COUNT 36

16. SUPPLEMENTARY NOTATION

17. COSATI CODES			18. SUBJECT TERMS (Continue on reverse if necessary and identify by block number)
FIELD	GROUP	SUB-GROUP	Probe theory, magnetic limiting, space charge

19. ABSTRACT (Continue on reverse if necessary and identify by block number)

We consider a high-voltage spherical probe with parameters representative of the SPEAR I rocket experiment in the ionospheric plasma. Computer simulations (using particle-tracking and Poisson solution) illustrate the compression of the sheath in the direction normal to the magnetic field, the nature of the particle trajectories, and the space charge structure in the sheath. It is found that for a cold, dense plasma, the sheath is nearly confined within the Parker-Murphy radius and the collected current is near the Parker-Murphy limit. If the plasma is warmer and less dense, the sheath expands beyond the Parker-Murphy radius and the collected current decreases.

In addition, we present a "modified orbit-limited" theory capable of reproducing many of the qualitative and quantitative features of the sheath structure without the need for particle-tracking.

20. DISTRIBUTION/AVAILABILITY OF ABSTRACT UNCLASSIFIED/UNLIMITED ☐ SAME AS RPT ☐ DTIC USERS	21. ABSTRACT SECURITY CLASSIFICATION Unclassified	
22a. NAME OF RESPONSIBLE INDIVIDUAL David L. Cooke	22b. TELEPHONE (Include Area Code) (617) 377-2931	22c. OFFICE SYMBOL AFGL/PHK

DD FORM 1473, JUN 86   Previous editions are obsolete   SECURITY CLASSIFICATION OF THIS PAGE

Current Collection by a High-Voltage Sphere
from a Cold Magnetoplasma

M. J. Mandell, M. Rotenberg, and I. Katz

S-CUBED Division of Maxwell Laboratories

1. Introduction

The objective of this work is to understand current collection by, and the potential and charge density around, a high voltage probe in an ionospheric plasma in the absence of scattering. As a canonical case, we have chosen a spherical probe 10 cm. in radius, held at a potential of 11,000 volts, in a plasma of density 10^{11} m^{-3}, and temperature 0.1 eV, with a magnetic field of 0.3 gauss. This plasma has a thermal current of 8.46×10^{-4} A-m^{-2} and a Debye length of 0.743 cm.

The best estimate for collected current in this regime is the Parker-Murphy limit,[1] which we discuss in Section 2. In Section 3 we describe the features of a computer code which we used to simulate this problem. Results for the canonical case and related cases are described in Section 4. Section 5 discusses the results of an orbit-limited theory for the charge density (and thus potential) about the probe. The theory itself is derived in an appendix. Conclusions are given in Section 6.

2. Parker-Murphy Limit

The Parker-Murphy limit[1] is derived by considering the maximum cylinder (about a field line through its center) from which a probe can draw current, consistent with conservation of energy and canonical angular momentum. The canonical angular momentum is given by

$$p_\theta = mr^2(d\theta/dt + \omega/2)$$

where

$$\omega = eB/m,$$

1. Parker, L. W. and B. L. Murphy, "Potential Buildup on an Electron-Emitting Ionospheric Satellite", Journal of Geophysical Research 72, 1631-1636 (1967).

and its associated kinetic energy by

$$(p_\theta - mr^2\omega/2)^2/2mr^2.$$

Neglecting the electron's kinetic energy at its maximum radius, R, and the r- and z-components of velocity at the probe radius, a, we find

$$e\phi = (mR^2\omega/2 - ma^2\omega/2)^2/2ma^2$$

or

$$R^2/a^2 = 1 + (8e\phi/m\omega^2a^2)^{1/2}.$$

The maximum current to the probe is then given by

$$2\pi J_{th}(R^2/a^2)$$

where

$$J_{th} = ne(e\theta/2\pi m)^{1/2}.$$

For the parameters of our canonical problem we have

$$\omega = 5.275\times10^6 \text{ sec}^{-1}$$
$$R = 1.54 \text{ m}$$
$$I_{PM} = 12.6 \text{ mA}.$$

3. Computational Method

We have developed a 2½ dimensional computer code (two-dimensional coordinates and three-dimensional velocities) to simulate this problem. The code operates in cylindrical (r, z, θ) coordinates on a quadrilateral grid consisting of 90 spherical shells extending from the probe surface (0.1 m) to a radius of 7 meters. Each shell had 25 angular divisions ranging from the z-axis to the r-axis. The z=0 plane was treated as a mirror plane, and the r=7m sphere was held fixed at zero potential.

Electrons were started along the magnetic field (z) direction from just inside the 7m sphere with a radial spacing of 2.3 cm., and with current and velocity set to reproduce the one-sided plasma thermal current and one-half the ambient density. (Beyond the collection radius, the remaining half of the ambient density comes from electrons reflected from the z=0 mirror plane.) Energy and canonical angular momentum were explicitly conserved at each particle timestep. Each electron was followed until it either (a) hit the

2

probe; (b) escaped the grid; or (c) exceeded the limit on how many times it was allowed to bounce off the mirror plane. At each timestep the particle's charge was bilinearly shared to the nearby gridpoints. Ion density was set to $ne^{-2\phi/\pi\theta}$.

Iterations consisted of alternately solving Poisson's equation and tracking particles in the resulting potentials to update the charge density. This process was continued until steady state solutions were achieved. Potentials were constrained to be non-negative, and in most runs charge densities were constrained to be non-positive. (The charge-density constraint affects potentials along field lines within the collection radius, which in the quasi-neutral limit satisfy

$$e^{-2\phi/\pi\theta} = 0.5 \, (1 + \pi \, \phi \, / \, \theta)^{-\frac{1}{2}}.$$

It had negligible effect on collected currents or on potentials beyond the collection radius.)

4. Computational Results and Discussion

Runs were done for the canonical set of parameters and for related parameters. A complete list of the runs with their results is found in Table I. Line 5 of Table I is our best solution for the canonical case. The canonical case is difficult because the Debye length is short compared to the mesh spacing used, and because the particle energy is tiny compared with the potential scale of the problem. Much insight can be gained by calculating comparable cases with higher energy. Lines 11 and 14 are our best solutions for comparable cases in which the plasma thermal current is the same as the canonical case, but the plasma temperature is raised to 1 and 10 eV respectively. The other cases are presented for illustrative purposes.

The general character of all runs is that (a) particles originating within a "collection radius" (somewhat less than the Parker-Murphy radius) are "promptly" (i.e., within three crossings of the z=0 mirror plane) collected by the probe; (b) most particles originating between the "collection radius" and the Parker-Murphy radius escape the sheath region; some are collected after executing lengthy trajectories; (c) there is a very substantial region extending outward from the Parker-Murphy radius whose particles are "trapped", i.e., escape the sheath only after very lengthy trajectories involving tens of crossings of the mirror plane; and (d) particles traversing only the outermost portion of the sheath are not trapped. How close the "collection radius" is to the Parker-Murphy radius is

3

determined primarily by the radial extent of the sheath, with longer-range potentials collecting smaller currents. Note that Table I is ordered by the radius at which the potential drops to 100 volts. The current collected is very strongly inversely correlated with this 100 volt radius.

The number of "bounces" (i.e., passages through the mirror plane) allowed affects the collected current both directly (i.e., a particle that initially missed the probe may eventually stumble into it), and indirectly. The indirect effect is that long trajectories accumulate a large charge density which reduces the extent of the sheath. These points are well illustrated by the runs shown in Table II, in which increased bounce number leads to more space charge, and thence to a more compact potential, more collected current, and less trapped current. Lines 16 and 17 of Table I are calculations performed using the Langmuir-Blodgett[2] (spherical space-charge limited) potential, which happens to be similar to the potential of line 15. In going from three bounces to 50 bounces (line 17 to line 16) the collected current increases from 4.6 to 7.6 mA, still well below the Parker-Murphy limit. However, even after 50 bounces 40 mA of current remains trapped. Taking into account the effect of the trapped charge on the potential (Table II) we get a larger increase (to 10 mA) of current, as the 100-volt contour moves in from 2.1 m to 1.4 m. Furthermore, we dispose of all but 6 mA of the trapped current.

Increasing the temperature reduces the collected current primarily through decreased shielding of the potential. Shielding is decreased because the lifetime of trapped particles is reduced, due to increased probability of escape. Increasing the plasma temperature from 0.1 to 1 to 10 eV (Table III) we find that the 100-volt contour moves outward from 1.4 to 1.6 to 2.0 meters, and the collected current decreases from 10 mA to 9 mA to 6 mA. Note that the current is reduced by the shape of the potential, rather than directly by the higher energy of the incident particles. Line 4 of Table I shows a 10 eV plasma with ten times the thermal current of the canonical case. Its potential profile is comparable to that of line 6, and its collected current scales directly with the plasma thermal current, despite a hundredfold increase in particle energy.

---

2. Langmuir, I. and K. B. Blodgett, "Currents Limited by Space Charge between Concentric Spheres", *Physical Review 24*, 49-59 (1924).

Runs which allowed positive charge density had positive potentials extending along the field lines within the collection radius. This had no effect on the collected current.

Figures 1 and 2 show the electrostatic potentials and particle trajectories for the 0.1 eV and 10 eV cases (lines 5 and 14 of Table I). (Note that the actual runs followed more trajectories for longer paths than shown in the figures.) The positive potentials extending along the field lines are seen clearly in the 10 eV case. Note also the line of "turning points" for particles which missed the sphere. These particles are actually orbiting the symmetry axis, and contributing substantially to the charge density. Both of these features are also present in the 0.1 eV case, but are difficult to see in the figure.

Figure 3 shows the charge density for the 0.1 eV case (Table I, line 5). Note that the charge density is relatively low in the region traversed by collected electrons, and higher in the trapping region. Figure 4 shows the charge density along a radial line normal to the magnetic field for all three temperatures. For all but the 10 eV case, there is a sharp peak in the charge density at a radius of about 0.4 m. This peak consists of electrons which originated just outside the Parker-Murphy radius. For a circular orbit at a given radius, the centrifugal force (outward) and the magnetic force (outward) on an electron are determined by conservation of orbital angular momentum. These do indeed balance the electric force (inward) at a radius of about 0.4 m. However, the kinetic energy associated with this circular motion is well under half the total kinetic energy of these electrons; most of their kinetic energy is associated with oscillations parallel to the magnetic field.

5. Orbit-Limited Theory

The appendix presents a theory for an upper bound to the charge density for this problem. By "orbit-limited" we mean that any point in phase-space whose energy and canonical momentum are consistent with a trajectory connecting to ambient plasma contributes to the local density. This is known to give a charge density which is far too high, because it contains contributions from trajectories which can reach a field point only in the presence of bizarrely unrealistic potentials. However, we can modify the orbit-limited theory as follows to assure that the charge density is built up from only "reasonable" trajectories.

5

We first note that trajectories originating within a "collection radius", R_1, are immediately collected by the probe. Therefore, we exclude this region of angular momentum from the orbit-limited charge density integrals, and instead treat such trajectories by accelerated current formulas. We also exclude particles outside some larger radius, R_2, which may be roughly interpreted as the "range of the potential", on the grounds that such particles never see any fields which draw them into the sheath region. Outside R_2 we use accelerated current formulas to determine electron density.

If we take the "range of the potential" to be the radius at which the potential drops to the plasma temperature, we can imagine solving the problem self-consistently using these "modified orbit-limited" charge densities. This can be done easily only for the case of the 10 eV plasma. We find that the resultant potential is qualitatively correct, but too compact, i.e., the charge density is still too high. It follows that the currents in this potential will be too high. Figure 5 shows the solution for the 10 eV case using the modified orbit-limited theory.

Alternatively, we can generate any reasonable set of potentials (either by using a particle tracking code or, for example, by solving Laplace's equation inside a grounded ellipse), set R_1 to be at or just inside the Parker-Murphy radius, and determine R_2 by the requirement that the total charge in the sheath cancel the charge on the sphere. (This method does not require that $R_2 - R_1$ be resolvable by the computer code.) Figure 6 shows charge densities calculated for the 0.1 eV case using the potentials of figure 1, R_1 = 1.54 m, and R_2 = 1.56 m. Comparing figure 6 with figure 3, we find that the theory gives a much sharper boundary between the high and low density regions, and that the theory does not predict the structure due to particle dynamics in the high density region. It can be shown (see appendix) that the theory predicts a density

$$\rho/\rho_0 = (m\omega^2 r^2/8\pi T)^{\frac{1}{2}} \times [(R_2^2 - R_1^2)/r^2]$$

for all points whose radius and potential are consistent with trajectories connecting to the spherical shell $R_1 < R < R_2$.

Table I includes results from the "modified orbit-limited" theory for the 0.1, 1, and 10 eV cases. Only in the 10 eV case is the answer truly self-consistent; the charge densities in the other two cases are too high to easily achieve self-consistency. However, these potentials follow the same theme of giving a potential which is too compact and draws more current than obtained by particle-tracking.

6

6. Conclusions

We have used a particle-tracking code to calculate potentials and currents associated with an 11 kV, 10 cm probe in an ionospheric plasma. We have also developed a "modified orbit-limited" theory which yields potentials about the probe which are qualitatively good, but quantitatively are too compact.

For fixed probe voltage and magnetic field, the probe current has a strong inverse correlation with the extent of the potential, i.e., longer-ranged potentials draw less current. The reason for this is that particles at a given radius receive more longitudinal acceleration, and less radial acceleration, as the potential becomes longer-ranged. Particles originating at the Parker-Murphy radius can hit the probe only with zero longitudinal velocity, and the probability of having a small longitudinal velocity when near the probe is less likely for a longer-ranged potential.

The range of the potential is determined by particles which are "trapped". Most of these originate in a region just outside the Parker-Murphy radius, and spend a large amount of time orbiting close to the probe. This is illustrated by figure 4, which plots the net charge density for the three cases. Note the very high (several times ambient density) peak in the charge density at about 0.4 m. This corresponds approximately to the radius of a circular orbit where electrostatic (inward), centrifugal (outward), and magnetic (outward) forces balance for electrons originating just outside the Parker-Murphy radius and moving in the (E×B) direction.

7

Table I.
Potential and Current Collection Calculations

#	V [V]	T [eV]	n [m^{-3}]	+Q Allowed	NBounce	I_{Col} [mA]	I_{Trap} [mA]	R(100) [m]	R(10) [m]	R(0.1) [m]
1	11,000(A)	0.1	1×10^{11}	n	23	11.7	5	1.0	1.45	1.9
2	11,000(B)	1.0	3×10^{10}	n	23	12.4	6	1.1	1.7	2.3
3	11,000(B)	1.0	3×10^{10}	y	-	-	-	1.1	1.7	2.4
4	11,000	10.	1×10^{11}	n	13	110	32	1.3	1.7	1.9
5	11,000	0.1	1×10^{11}	y	50	ι0	6	1.4	1.8	1.9
6	11,000	0.1	1×10^{11}	n	50	11	9	1.4	1.8	2.0
7	11,000	0.1	1×10^{11}	n	20	9.0	22	1.5	1.9	2.0
8	11,000(C)	10.	1×10^{10}	n	23	7.3	7.2	1.5	2.2	3.2
9	11,000(C)	10.	1×10^{10}	y	23	-	-	1.7	2.6	3.6
10	11,000	1.	3×10^{10}	n	23	8.0	8.0	1.6	2.1	2.3
11	11,000	1.	3×10^{10}	y	23	9.0	5.0	1.6	2.1	2.4
12	11,000	10.	1×10^{10}	n	23	6.5	3	1.7	2.2	2.9
13	11,000	0.1	1×10^{11}	n	10	6.7	30	1.8	2.4	2.7
14	11,000	10.	1×10^{10}	y	50	6.8	0	1.95	2.7	4.5
15	11,000	0.1	1×10^{11}	n	3	4.2	46	2.1	2.8	3.5
16	11,000(D)	0.1	1×10^{11}	-	50	7.6	40	2.2	2.9	3.5
17	11,000(D)	0.1	1×10^{11}	-	3	4.6	46	2.2	2.9	3.5

(A) Modified orbit-limited charge density ; (R1,R2)=(1.40,1.46).
(B) Modified orbit-limited charge density ; (R1,R2)=(1.50,2.10).
(C) Modified orbit-limited charge density ; (R1,R2)=(1.13,2.20).
(D) Langmuir-Blodgett Potential.

Table II.
Effects of "bounce number" on the potential
and collected current calculated for the probe.

#	V	T	n	+Q	NBounce	I_{Col}	L_{Trap}	R(100)	R(10)	R(0.1)
-	[V]	[eV]	[m^{-3}]	Allowed	-	[mA]	[mA]	[m]	[m]	[m]
5	11,000	0.1	1×10^{11}	n	50	11	9	1.4	1.8	2.0
7	11,000	0.1	1×10^{11}	n	20	9.0	22	1.5	1.9	2.0
13	11,000	0.1	1×10^{11}	n	10	6.7	30	1.8	2.4	2.7
15	11,000	0.1	1×10^{11}	n	3	4.2	46	2.1	2.8	3.5

Table III.
Effects of increasing temperature (at constant
current density) on the potential and collected current.

#	V	T	n	+Q	NBounce	i_{Col}	L_{Trap}	R(100)	R(10)	R(0.1)
-	[V]	[eV]	[m^{-3}]	Allowed	-	[mA]	[mA]	[m]	[m]	[m]
5	11,000	0.1	1×10^{11}	y	50	10	6	1.4	1.8	1.9
11	11,000	1.	3×10^{10}	y	23	9.0	5.0	1.6	2.1	2.4
14	11,000	10.	1×10^{10}	y	50	6.8	0	1.95	2.7	4.5

Figure Captions

Figure 1. Electrostatic potential contours (solid lines) and particle trajectories (dotted lines) for a 0.1 meter radius sphere at 11 kV, magnetic field 0.3 gauss, plasma density 10^{11} m^{-3}, plasma temperature 0.1 eV. Contours are logarithmically spaced, with the outermost contour at 1 volt. The figure has mirror symmetry at the R-Axis and rotational symmetry about the Z-Axis. Distances are noted in meters.

Figure 2. Electrostatic potential contours (solid lines) and particle trajectories (dotted lines) for a 0.1 meter radius sphere at 11 kV, magnetic field 0.3 gauss, plasma density 10^{10} m^{-3}, plasma temperature 10 eV. Contours are logarithmically spaced, with the outermost contour at 1 volt. The figure has mirror symmetry at the R-Axis and rotational symmetry about the Z-Axis. Distances are noted in meters.

Figure 3. Charge density for a 0.1 meter radius sphere at 11 kV, magnetic field 0.3 gauss, plasma density 10^{11} m^{-3}, plasma temperature 0.1 eV. (Compare potentials and trajectories, figure 1.) The contours are logarithmically spaced and denote the negative of the charge density (ρ/ε_0); ambient is 1807. Note the low charge density along the Z-Axis, the sharp peak on the R-Axis at R = 0.5 meters, and the ridge extending upward from the R-Axis just inside the sheath.

Figure 4. Charge density (ρ/ε_0) for the 0.1 eV case (curve with two sharp peaks, ambient = 1807, compare fig. 3), 1.0 eV case (curve with two broad peaks, ambient = 571), and the 10 eV case (flat curve, ambient = 181).

Figure 5. Electrostatic potentials and particle trajectories for a 0.1 meter radius sphere at 11 kV, magnetic field 0.3 gauss, plasma density 10^{10} m^{-3}, plasma temperature 10 eV, calculated by the "modified orbit-limited theory". (Compare with figure 2.)

Figure 6. Charge densities calculated for the 0.1 eV case using the potentials of figure 1, R_1 = 1.54 m, and R_2 = 1.56 m. (Compare with figure 3.)
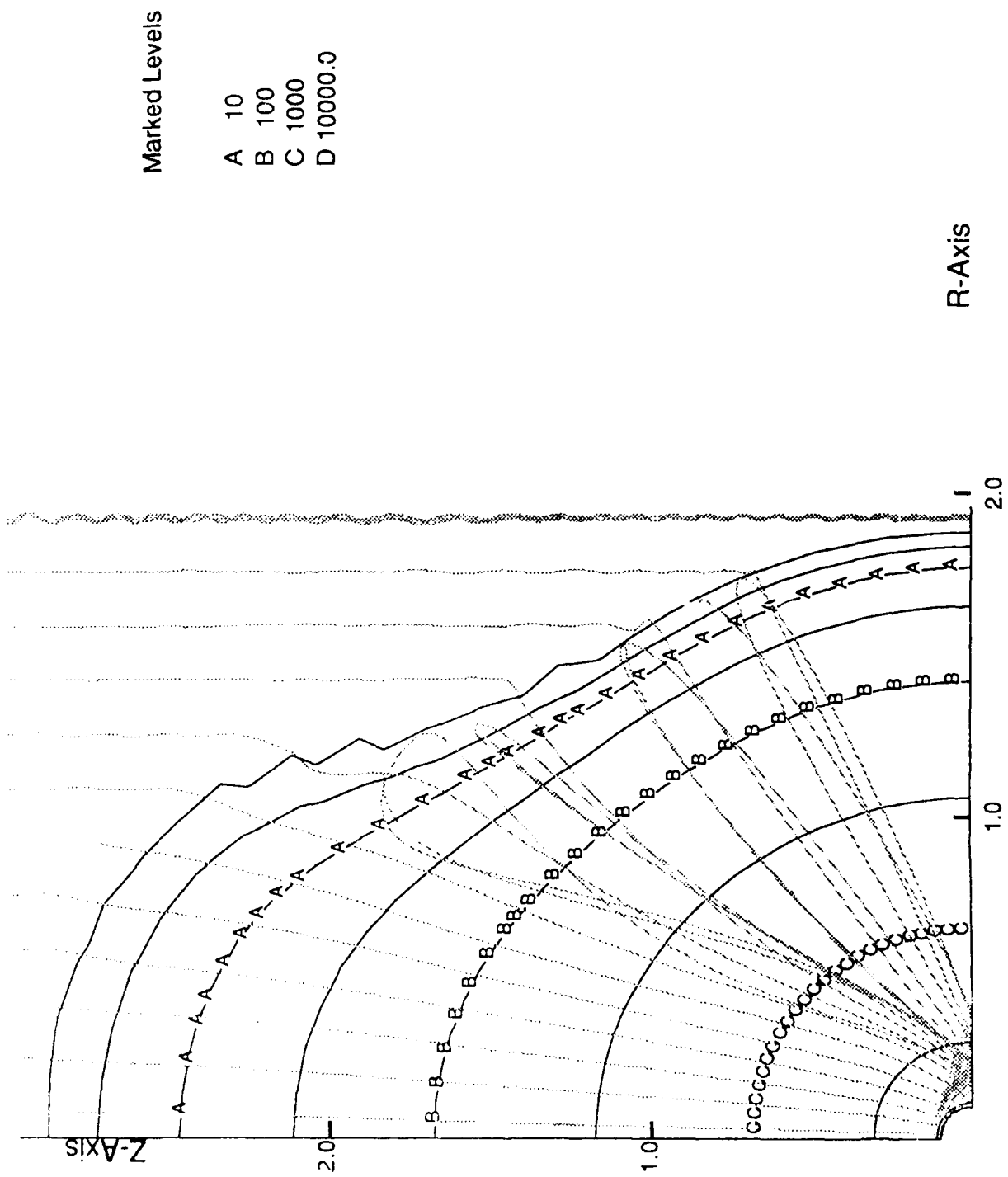
Marked Levels

A   10
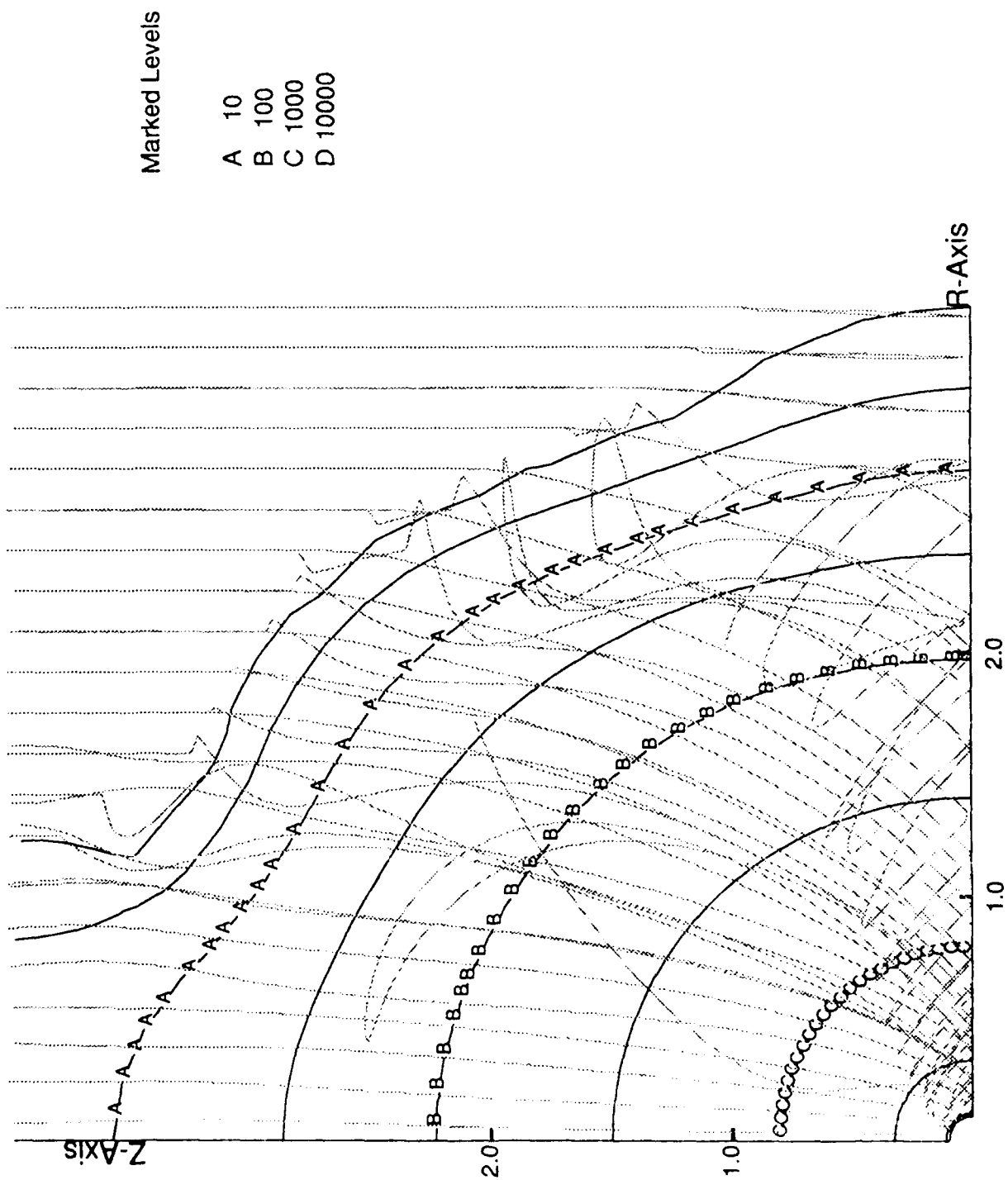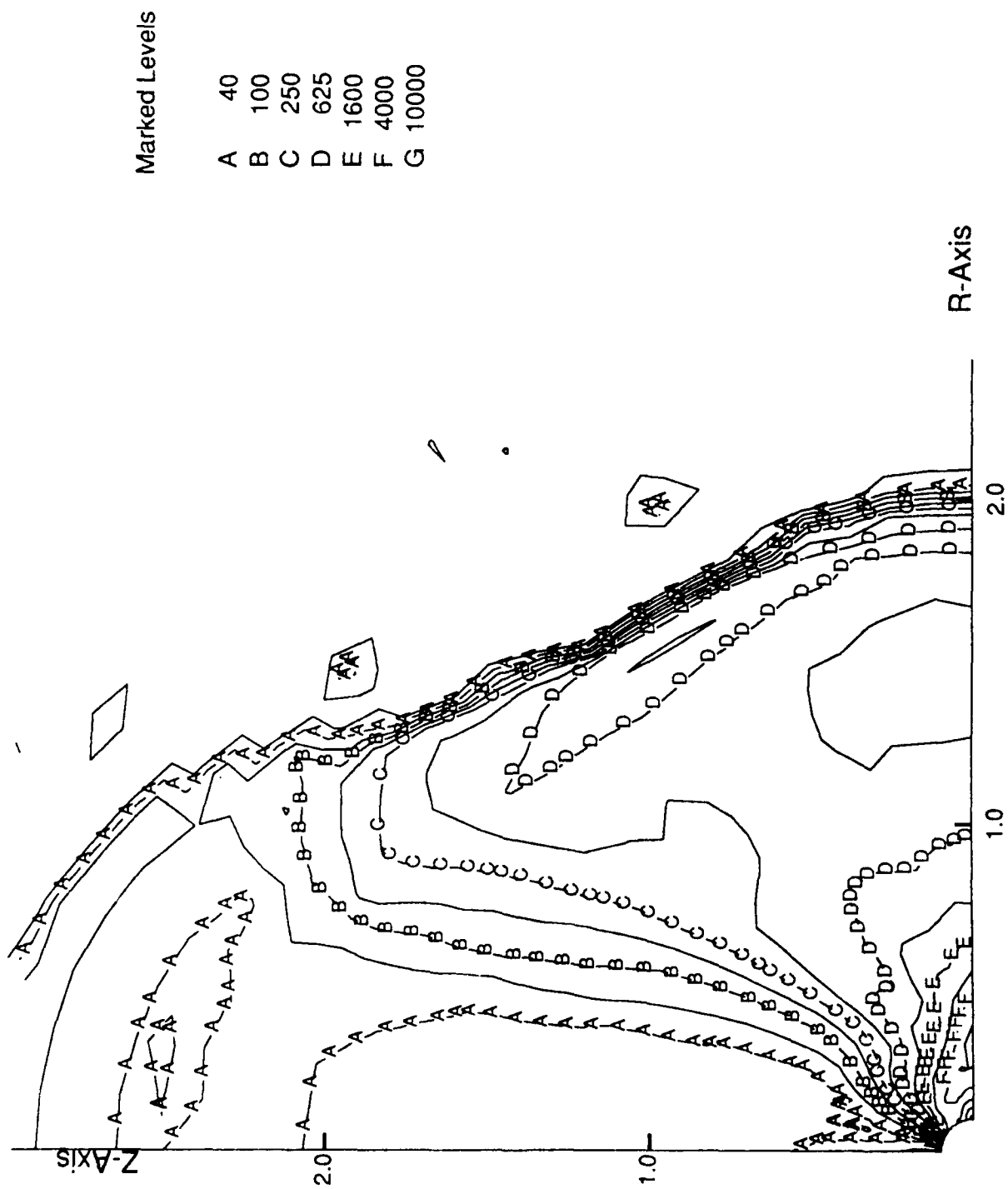B   100
C   1000
D   10000.0

R-Axis

Figure 1

11

Marked Levels

A 10
B 100
C 1000
D 10000

R-Axis

Z-Axis

2.0

1.0

1.0

2.0

Figure 2

12

Marked Levels

A 40
B 100
C 250
D 625
E 1600
F 4000
G 10000

R-Axis

Z-Axis

Figure 3

Charge Density

Radius

Figure 4

14

Marked Levels

A 10
B 100
C 1000
D 10000

R-Axis

Z-Axis

2.0

1.0

2.0

1.0

Figure 5

15

Marked Levels
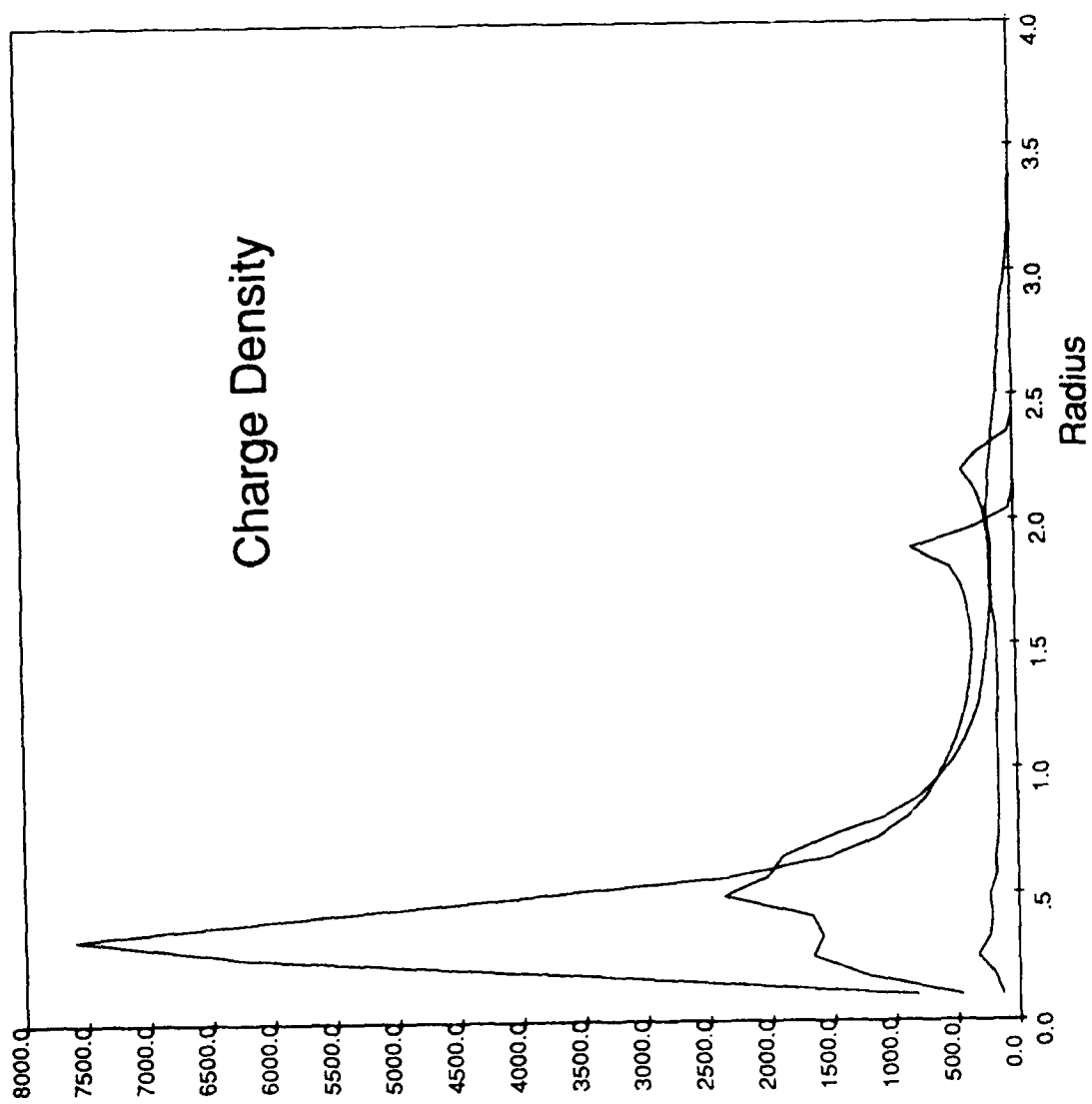
A 40
B 100
C 250
D 625
E 1600
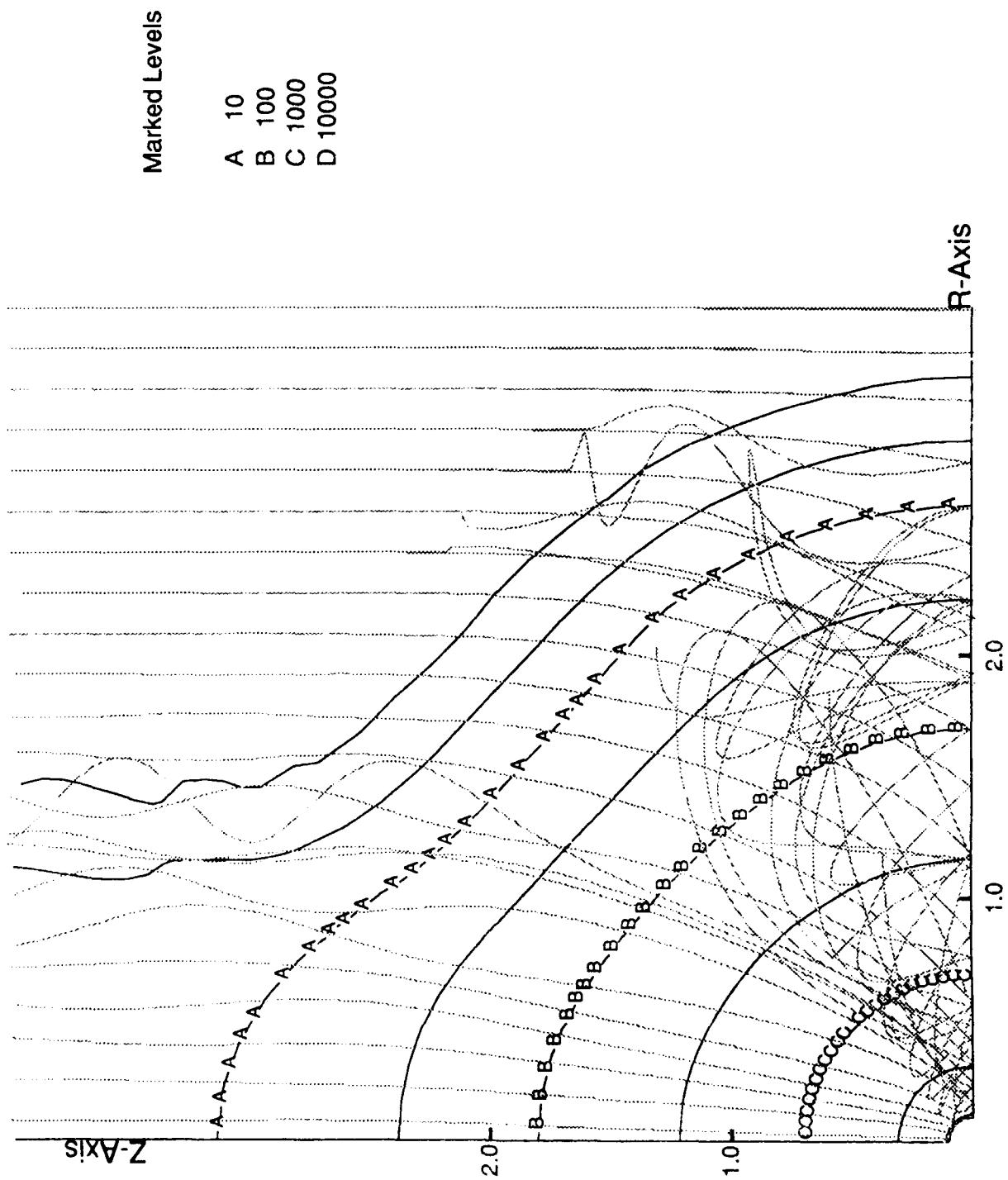F 4000
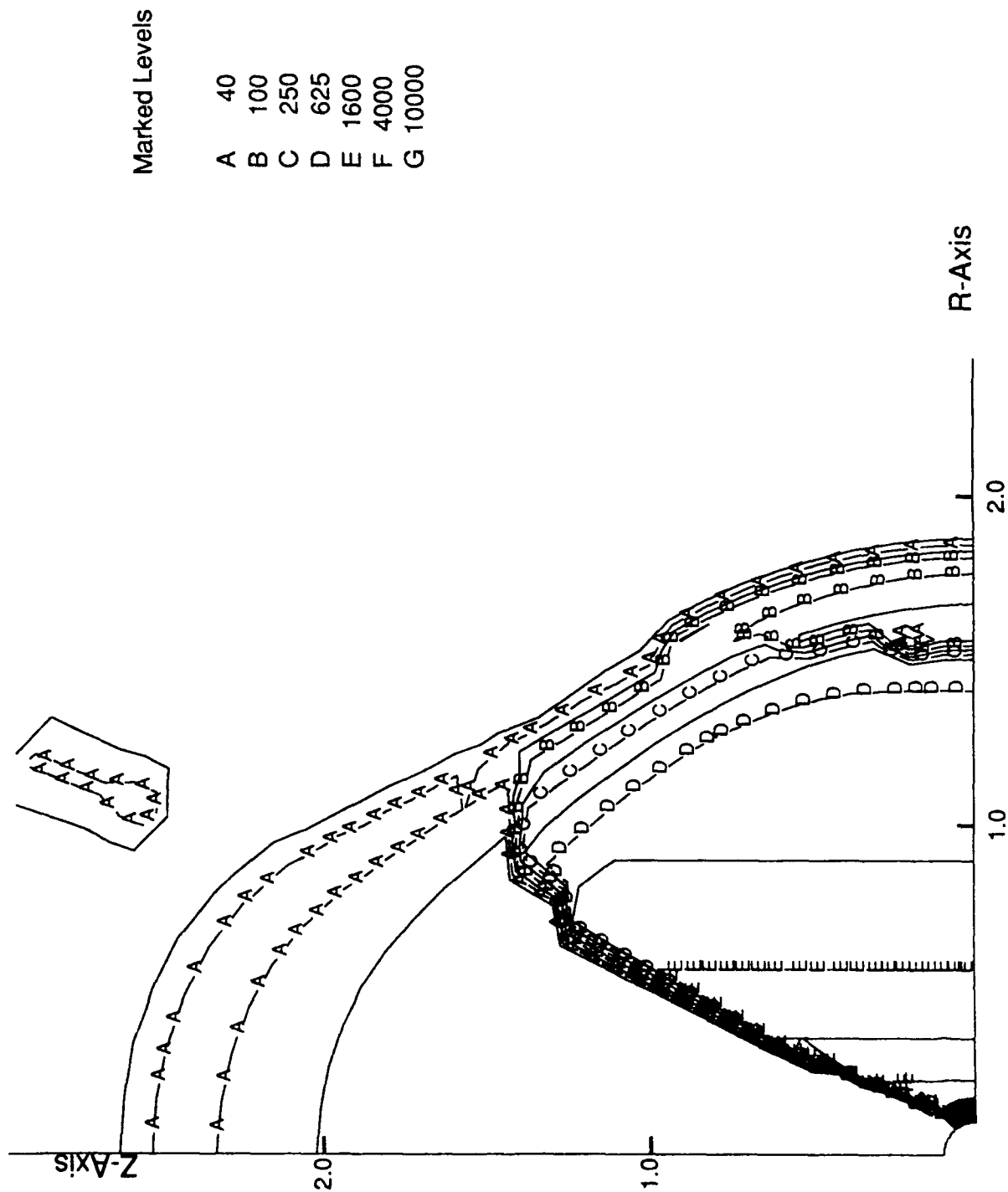G 10000

R-Axis

Figure 6

16

APPENDIX

ORBIT-LIMITED CHARGE DENSITY

IN MAGNETIC FIELD

Orbit-Limited Charge Density in Magnetic Field

With cylindrical coordinates, B-field along Z, the Lagrangian is

$$L = \frac{m}{2} \left(\dot{r}^2 + \dot{z}^2 + r^2\dot{\phi}^2 \right) + e\phi(r,z) + eB \frac{r^2}{2} \dot{\theta}$$

The canonical moments are $[\omega = \omega_c = eB/m]$

$$p_\theta = mr^2\dot{\theta} + eBr^2/2 = mr^2(\dot{\theta} + \omega/2)$$

$$p_r = m\dot{r}$$

$$p_z = m\dot{z}$$

The energy is

$$E = U + \frac{1}{2mr^2} \left(p_\theta - mr^2\omega/2 \right)^2 - e\,\phi(r,z)$$

where $U = \frac{1}{2m} \left(p_r^2 + p_z^2 \right)$

$$dp_r dp_z = 4\pi m\, dU$$

We need to relate the distribution factor, $f(r,z,\theta,p_r,p_z,p_\theta)$ to the ordinary density. Over some region we have

$$N = \int_\Omega \rho(r,z,\theta)\, r\, dr\, dz\, d\theta = \int_\Omega dr\, dz\, d\theta \int_\Psi dp_r dp_z dp_\theta\ f$$

so that $\displaystyle \int_\Psi f\, dp_r dp_z dp_\theta = r\rho$

In undisturbed plasma, the distribution function is

$$f_o(R, z_o, \theta, U_o, p_\theta) = \rho_o \left(2\pi m T^3\right)^{-1/2} \exp^{-U_o/T}$$

$$\times \exp^{-(p_\theta - mR^2\omega/2)^2/2mR^2T}$$

I.   Non-Magnetized Case

To do the nonmagnetized case, we set $\omega = 0$.

From a point (r, z, θ) within the sheath, trace an orbit back to a cylinder of radius R, where R lies beyond the range of the sheath. Then

$$\frac{r\rho(r)}{R\rho(R)} = \int_{-\infty}^{\infty} dp_\theta \int_{U_1}^{\infty} dU \left(2\pi m R^2 T^3\right)^{-1/2} e^{-\left(U_o + \frac{p_\theta^2}{2mR^2}\right)/T}$$

where the energy

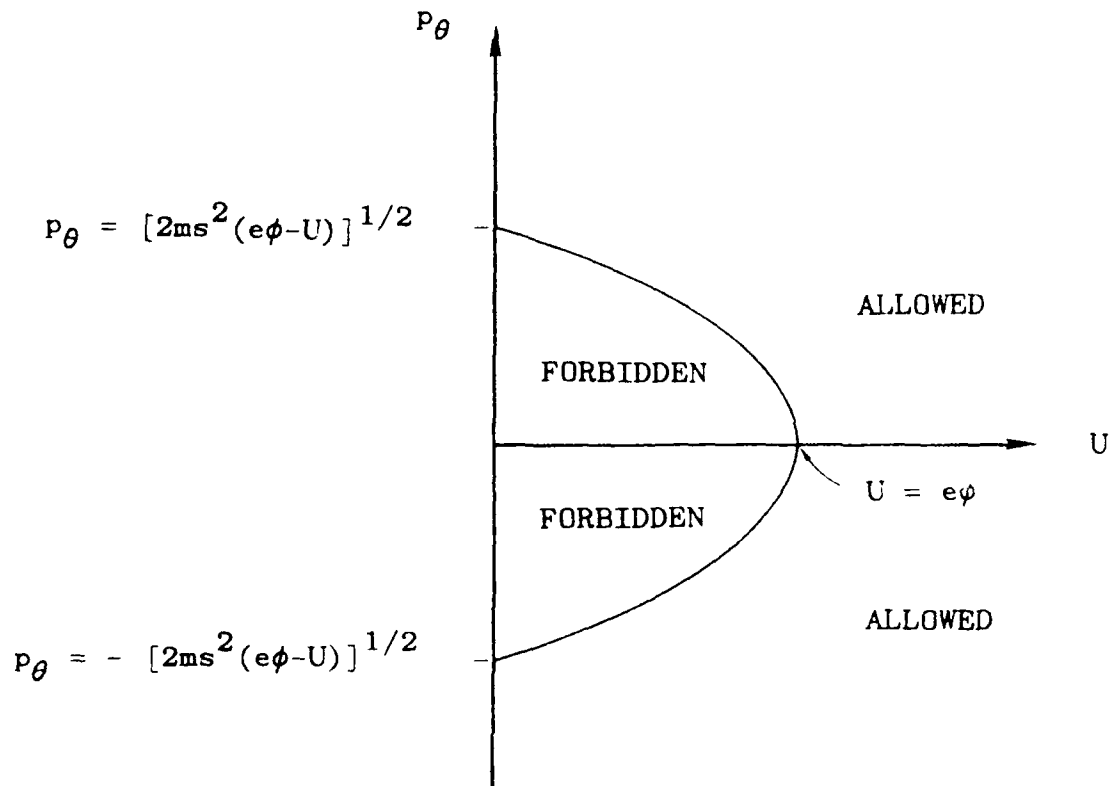$$E = U_o + p_\theta^2/2mR^2 = U - e\phi + p_\theta^2/2mr^2 > 0$$

$$\text{and } E > p_\theta^2/2mR^2$$

so that
$$U_1 = \frac{p_\theta^2}{2mR^2} - \frac{p_\theta^2}{2mr^2} + e\phi$$

and
$$\frac{r\rho(r)}{R\rho(R)} = \int_{-\infty}^{\infty} dp_\theta \int_{e\phi - p_\theta^2/2ms^2}^{dU} \exp\left[\left(e\phi - U - \frac{p_\theta^2}{2mr^2}\right)/T\right] \times \left(2\pi mR^2/T^3\right)^{-1/2}$$

where $\frac{1}{s^2} = \frac{1}{r^2} - \frac{1}{R^2}$.

Region of integration ($\omega = eB/m = 0$).

$p_\theta = [2ms^2(e\phi - U)]^{1/2}$

ALLOWED

FORBIDDEN

U

FORBIDDEN

$U = e\varphi$

ALLOWED

$p_\theta = -[2ms^2(e\phi - U)]^{1/2}$

The space within the parabola is "forbidden," i.e., these orbits do not connect to ambient. Changing the order of integrations, we have

$$\frac{r\rho(r)}{R\rho(R)} = \int_0^\infty dU \left(2\pi m R^2 T^3\right)^{-1/2} \exp\left[(e\phi - U/T\right] \int_{-\infty}^\infty dp_\theta \, \exp^{-p_\theta^2/2mr^2 T}$$

$$- \int_0^{e\phi} dU \left(2\pi m R^2 T^3\right)^{-1/2} \exp\left[(e\phi - U)/T\right] \int_{-\sqrt{2ms^2(e\phi-U)}}^{\sqrt{2ms^2(e\phi-U)}} dp_\theta \exp(-p_\theta^2/2mr^2 T)$$

$$= \frac{r}{R} \exp[e\phi/T] - \frac{r}{R} \int_0^{e\phi} \frac{dU}{T} \exp\left[(e\phi - U)/T\right] \mathrm{erf}\left[\frac{s}{r}\left(\frac{e\phi - U}{T}\right)^{\frac{1}{2}}\right]$$

Let $R \to \infty$, $(s/r) \to 1$

The integral becomes

$$- \int_{\frac{e\phi}{T}}^0 dx \, e^x \mathrm{erf}\left(x^{\frac{1}{2}}\right)$$

$$= \left[\mathrm{erf}\left(x^{\frac{1}{2}}\right) e^x - \left(\frac{4x}{\pi}\right)^{\frac{1}{2}}\right]_0^{e\phi/T}$$

so that

$$\frac{\rho}{\rho_O} = e^{e\phi/T}\left\{1-\mathrm{erf}\left[\left(\frac{e\phi}{T}\right)^{\frac{1}{2}}\right]\right\} + \left(\frac{4e\phi}{\pi T}\right)^{\frac{1}{2}}$$

Using $\mathrm{erf}(z) = 1 - e^{-z^2}/z\sqrt{\pi}$,

$$\frac{\rho}{\rho_O} = \left[T/\pi e\phi\right]^{\frac{1}{2}} + \left[4e\phi/\pi T\right]^{\frac{1}{2}} = 2\left(\frac{e\phi}{\pi T}\right)^{\frac{1}{2}}\left[1 + \left(\frac{T}{2e\phi}\right)\right]$$

for $e\phi/T \gg 1$. For $e\phi/T \ll 1$, we get

$$\frac{\rho}{\rho_O} = 1 + (e\phi/T) + 0\left[(e\phi/T)^2\right] \quad .$$

II. Magnetic Case

$$\omega = \frac{eB}{m} \neq 0$$

As before, we have

$$(2\pi mT^3)^{1/2} r\rho(r) = \int_{-\infty}^{\infty} dp_\theta \int_{e\phi\,-\,\frac{(p_\theta-mr^2\omega/2)^2}{2mr^2}\,+\,\frac{(p_\theta-mR^2\omega/2)^2}{2mR^2}}^{\infty} dU\,\rho(R)\exp\left[-\frac{1}{T}\left(e\phi-U-\frac{(p_\theta-mr^2\omega/2)^2}{2mr^2}\right)\right]$$

Now, we need a new criterion for R, the radius at which we terminate outwardly tracked orbits. Orbits with $p_\theta > 0$ do not include the r=0 axis. We terminate these orbits with

$$\dot{\theta} = 0$$

$$R^2 = 2\ p_\theta/m\omega$$

$$\frac{\left(p_\theta - mR^2\omega/2\right)^2}{2mR^2} = 0$$

Orbits with $p_\theta < 0$ do include the r=0 axis; for these:

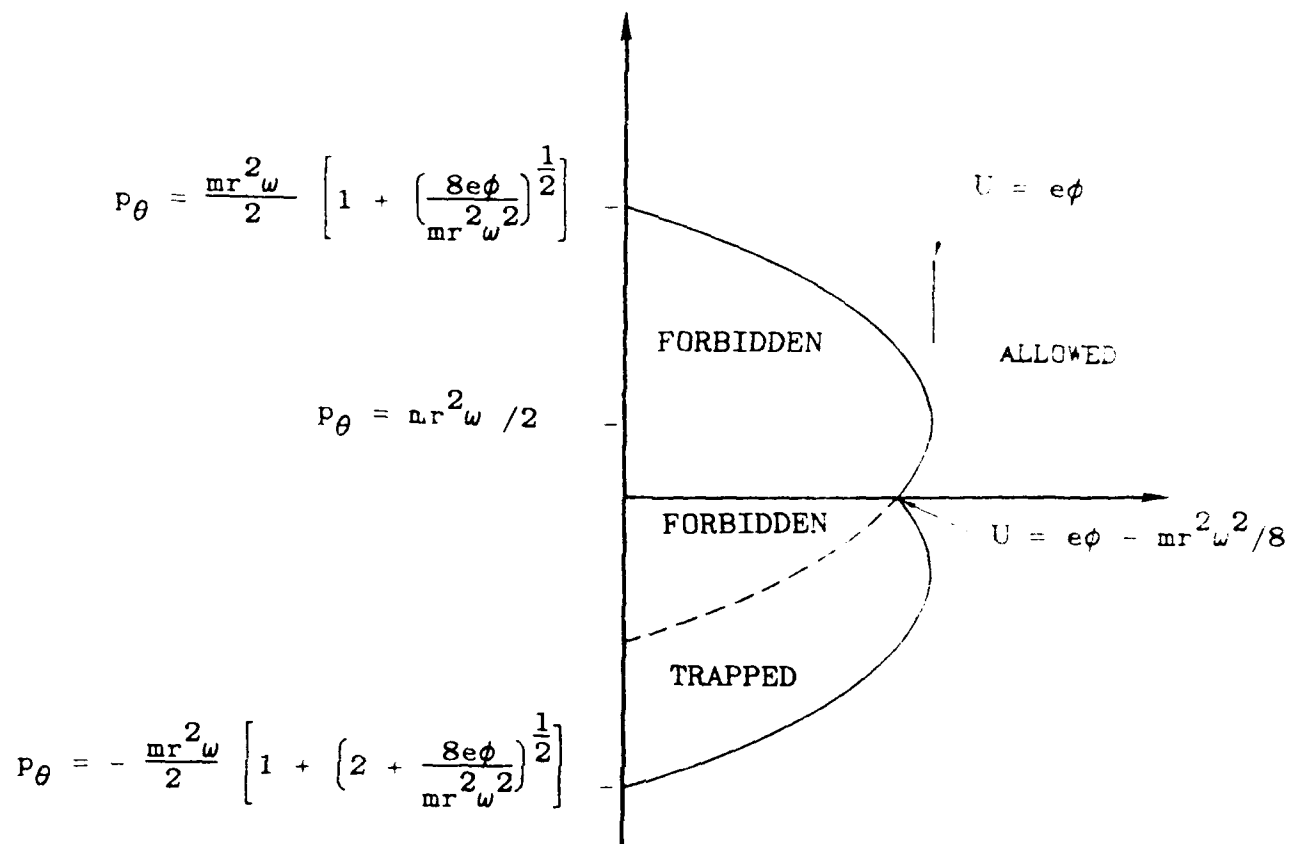$$\dot{\theta} = -\omega$$

$$R^2 = -2p_\theta/m\omega$$

$$\frac{\left(p_\theta - mR^2\omega/2\right)^2}{2mR^2} = -\ \omega p_\theta \qquad .$$

The region of integration is

$$U > \begin{cases} e\phi\ -\ \dfrac{\left(p_\theta - mr^2\omega/2\right)^2}{2mr^2} & (p_\theta > 0) \\[3em] e\phi\ -\ \dfrac{\left(p_\theta - mr^2\omega/2\right)^2}{2mr^2}\ -\ \omega p_\theta & (p_\theta < 0) \end{cases}$$

$$p_\theta = \frac{mr^2\omega}{2}\left[1 + \left(\frac{8e\phi}{mr^2\omega^2}\right)^{\frac{1}{2}}\right]$$

$$p_\theta = mr^2\omega /2$$

$$U = e\phi$$

FORBIDDEN

ALLOWED

FORBIDDEN

$$U = e\phi - mr^2\omega^2/8$$

TRAPPED

$$p_\theta = -\frac{mr^2\omega}{2}\left[1 + \left(2 + \frac{8e\phi}{mr^2\omega^2}\right)^{\frac{1}{2}}\right]$$

$$(2\pi mT^3)^{1/2}{}_r\rho(r)/\rho(R) = \int_0^\infty dU \int_{-\infty}^\infty dp_\theta \exp\left[\left(e\phi - U - \frac{(p_\theta - mr^2\omega/2)^2}{2mr^2}\right)/T\right]$$

$$\int_0^{e\phi - mr^2\omega^2/8} dU \int_0^{\frac{mr^2\omega}{2}[1 + (8(e\phi - U)/mr^2\omega^2)^{1/2}]} dp_\theta \exp[\cdots]$$

24

$$-\int_{e\phi-mr^2\omega^2/8}^{e\phi} dU \int_{\frac{mr^2\omega}{2}\left[1-\left(8(e\phi-U)/mr^2\omega^2\right)^{\frac{1}{2}}\right]}^{\frac{mr^2\omega}{2}\left[1+\left(8(e\phi-U)/mr^2\omega^2\right)^{1/2}\right]} dp_\theta \ \exp\ [\bullet\bullet\bullet]$$

$$-\int_{0}^{e\phi\ -mr^2\omega^2/8} dU \int_{-\frac{mr^2\omega}{2}\left[1+\left(8(e\phi-U)/mr^2\omega^2\right)^{\frac{1}{2}}\right]}^{0} dp_\theta \ \exp\ [\bullet\bullet\bullet]$$

$$-\int_{e\phi-mr^2\omega^2/8}^{e\phi} dU \int_{-\frac{mr^2\omega}{2}\left[1+\left(8(e\phi-U)/mr^2\omega^2\right)^{\frac{1}{2}}\right]}^{-\frac{mr^2\omega}{2}\left[1-\left(8(e\phi-U)/mr^2\omega^2\right)^{1/2}\right]} dp_\theta \ \exp\ [\bullet\bullet\bullet]$$

First term gives

$$\frac{r\rho(r)}{\rho_o} = r \ \exp(e\phi/T)$$

Second term gives

$$-\frac{r}{2}\int_{o}^{e\phi-mr^2\omega^2/8} \frac{dU}{T} \ e^{(e\phi-U)/T} \left[erf\left(\frac{e\phi-U}{T}\right)^{\frac{1}{2}} + erf\left(\frac{mr^2\omega^2}{8T}\right)^{\frac{1}{2}}\right]$$

Third term gives

$$
- r \int_{e\phi \, - \, \frac{mr^2\omega^2}{8}}^{e\phi} \frac{dU}{T} \, e^{(e\phi-U)/T} \, \mathrm{erf}\left(\frac{e\phi-U}{T}\right)^{\frac{1}{2}}
$$

Fourth term gives

$$
- \frac{r}{2} \int_{0}^{e\phi-mr^2\omega^2/8} \frac{dU}{T} \, e^{(e\phi-U)/T} \left[-\mathrm{erf}\left(\frac{mr^2\omega^2}{8T}\right)^{\frac{1}{2}} \right.
$$

$$
\left. + \, \mathrm{erf}\left[\left(\frac{mr^2\omega^2}{2T}\right)^{\frac{1}{2}} \left(1 + \left(\frac{2(e\phi-U)}{mr^2\omega^2}\right)^{\frac{1}{2}}\right)\right] \right]
$$

Fifth term gives

$$
- \frac{r}{2} \int_{e\phi-mr^2\omega^2/8}^{e\phi} e^{(e\phi-U)/T} \, \frac{dU}{T} \left[\mathrm{erf}\left[\left(\frac{mr^2\omega^2}{2T}\right)^{\frac{1}{2}} \left(1 + \left(\frac{2(e\phi-U)}{mr^2\omega^2}\right)1/2\right)\right] \right.
$$

$$
\left. - \, \mathrm{erf}\left[\left(\frac{mr^2\omega^2}{2T}\right)^{\frac{1}{2}} \left(1 - \left(\frac{2(e\phi-U)}{mr^2\omega^2}\right)^{\frac{1}{2}}\right)\right] \right]
$$

26

Gathering terms, we have

$$\frac{\rho(r)}{\rho_o} = \exp\ (e\phi/T)$$

$$-\int_0^{e\phi} \frac{dU}{T}\ e^{(e\phi-U)/T}\ \mathrm{erf}\left(\frac{e\phi-U}{T}\right)^{1/2}$$

$$+\frac{1}{2}\int_0^{e\phi-mr^2\omega^2/8} \frac{dU}{T}\ e^{(e\phi-U)/T}\ \mathrm{erf}\left(\frac{e\phi-U}{T}\right)^{1/2}$$

$$-\frac{1}{2}\int_0^{e\phi} \frac{dU}{T}\ e^{(e\phi-U)/T}\ \mathrm{erf}\left[\left(\frac{mr^2\omega^2}{2T}\right)^{\frac{1}{2}}\left(1+\left(\frac{2(e\phi-U)}{mr^2\omega^2}\right)^{\frac{1}{2}}\right)\right]$$

$$+\frac{1}{2}\int_{e\phi-\frac{mr^2\omega^2}{8}}^{e\phi} \frac{dU}{T}\ e^{(e\phi-U)/T}\ \mathrm{erf}\left[\left(\frac{mr^2\omega^2}{2T}\right)^{\frac{1}{2}}\left(1-\left(\frac{2(e\phi-U)}{mr^2\omega^2}\right)^{\frac{1}{2}}\right)\right]$$

The first two terms given the B=0 result. In the remaining
terms, the leading term of erf (1) cancels.

Expanding erf, we get

27

Term 3:

$$-\frac{1}{2\sqrt{\pi}} \int_{0}^{e\phi-mr^2\omega^2/8} \frac{dU}{T} \left(\frac{e\phi-U}{T}\right)^{-1/2}$$

$$= +\frac{1}{\sqrt{\pi}} \left[\left(\frac{mr^2\omega^2}{8T}\right)^{\frac{1}{2}} - \left(\frac{\phi}{T}\right)^{\frac{1}{2}} \right]$$

Term 4:

$$+\frac{1}{2\sqrt{\pi}} \int_{0}^{e\phi} \frac{dU}{T} \ e^{-\left(\frac{mr^2\omega^2}{2T} + 2\left(\frac{e\phi-U}{T}\right)^{\frac{1}{2}}\left(\frac{mr^2\omega^2}{2T}\right)^{\frac{1}{2}}\right)}$$

$$\times \ \left(\frac{mr^2\omega^2}{2T}\right)^{-1/2} \left(1+\left(\frac{2(e\phi-U)}{mr^2\omega^2}\right)^{1/2}\right)^{-1}$$

$$= +\frac{1}{2\sqrt{\pi}} \left[\left(\frac{mr^2\omega^2}{2T}\right)^{\frac{1}{2}} e^{-mr^2\omega^2/2T} \right.$$

$$\int_{0}^{e\phi} \frac{e^{-2[(e\phi-U)(mr^2\omega^2)/2T^2]^{1/2}}}{1+\left[\frac{2(e\phi-U)}{mr^2\omega^2}\right]^{1/2}} \frac{dU}{T}$$

$$= \text{small}$$

28

Term 5:
$$-\frac{1}{2\sqrt{\pi}} \int_{e_{\uparrow}^{-\frac{mr^2\omega^2}{8}}}^{e\phi} \frac{\frac{dU}{T} \, e^{-\left(\frac{mr^2\omega^2}{2T} - [2(e\phi-U)(mr^2\omega^2)/T^2]^{\frac{1}{2}}\right)}}{\left(mr^2\omega^2/2T\right)^{\frac{1}{2}} - \left((e\phi-U)/T\right)^{\frac{1}{2}}}$$

(steps omitted)

$$= -\frac{1}{4\sqrt{\pi}} \times \left(\frac{2T}{mr^2\omega^2}\right)^{\frac{1}{2}}$$

So, finally,

$$\frac{\rho}{\rho_0} = \left(\frac{T}{\pi e\phi}\right)^{1/2} + \frac{1}{\sqrt{\pi}}\left[\left(\frac{e\phi}{T}\right)^{1/2} + \left(\frac{mr^2\omega^2}{8T}\right)^{1/2}\right]$$

III.   A More Reasonable Orbit-Limit.

We can get a more reasonable orbit-limited bound on density by noting that:

a) Particles originating within radius R_1, hit the object, and contribute negligibly to the density;

b) Particles originating outside radius R_2 (the range of the potential) may be ignored, as they never see the potential; and

c) We also ignore orbiting particles ($p_\theta < 0$).

Define

$$P_1 = mR_1^2\,\omega/2$$

$$P_2 = mR_2^2\,\omega/2$$

$$P_{max} = mr^2\,\omega/2\,\left[1 + \left(8e\phi/mr^2\omega^2\right)^{1/2}\right]$$

$$P_{min} = \max\left(0, mr^2\omega/2\,\left[1 - \left(8e\phi/mr^2\omega^2\right)^{1/2}\right]\right)\quad.$$

From above we have

$$\frac{\rho(r,\phi)}{\rho_o} = \left(2\pi mr^2 T^3\right)^{-1/2}\int_{P_1}^{P_2} dp_\theta$$

$$\times \int_{\max\left(0, e\phi - \frac{\left(p_\theta - mr^2\omega/2\right)^2}{2mr^2}\right)}^{\infty} dU\,\exp\left[\left(e\phi - U - \left(p_\theta - mr^2\omega/2\right)^2/2mr^2\right)/T\right]\quad.$$

Case A: $\quad P_2 > P_1 > P_{max}$

Leads to

$$\frac{\rho_A(r,\phi)}{\rho_o} = \frac{1}{2}\,e^{\,e\phi/T}\,\left[\,\mathrm{erf}\left(\frac{P_2 - mr^2\omega/2}{\left(2mr^2 T\right)^{1/2}}\right)\right.$$

$$\left. - \,\mathrm{erf}\left(\frac{P_1 - mr^2\omega/2}{\left(2mr^2 T\right)^{1/2}}\right)\,\right]$$

If the arguments of erf are large, we may use the asymptotic expansion to write

$$\frac{P_2 - mr^2\omega/2}{\left(2mr^2T\right)^{1/2}} = \frac{P_2 - P_{max}}{\left(2mr^2T\right)^{1/2}} + \left(\frac{e\phi}{T}\right)^{1/2}$$

$$\frac{1}{2} e^{\phi/T} erfc \left[\frac{P_2 - mr^2\omega/2}{\left(2mr^2T\right)^{1/2}}\right] = \frac{1}{2\sqrt{\pi}} \left[\frac{\left(2mr^2T\right)^{1/2}}{P_2 - mr^2\omega/2}\right]$$

$$\times \exp\left[-\frac{(P_2 - P_{max})}{\left(2mr^2T\right)^{1/2}} \left[\frac{(P_2 - P_{max})}{\left(2mr^2T\right)^{1/2}} + 2\left(\frac{e\phi}{T}\right)^{1/2}\right]\right]$$

(and similarly for P_1 terms) .

Case B: $P_{max} > P_2 > P_1 > mr^2\omega/2 \left[1 - \left(\frac{8e\phi}{mr^2\omega^2}\right)^{1/2}\right]$

In this case the inner integral simply gives T, so we

$$\frac{\rho_B(r,\phi)}{\rho_0} = \left(\frac{m\omega^2 r^2}{8\pi T}\right)^{1/2} \left[\frac{R_2^2 - R_1^2}{r^2}\right]$$

$$= \left(\frac{1}{2\pi mr^2 T}\right)^{1/2} (P_2 - P_1)$$

Case C: $mr^2\omega/2 \left[1 - \left(\frac{8e\phi}{mr^2\omega^2}\right)^{1/2}\right] > P_2$

This is similar to Case A, giving

$$\frac{\rho_C(r,\phi)}{\rho_o} = \frac{1}{2} \circ e^{\phi/T} \left[\mathrm{erf} \left(\frac{mr^2\omega/2 - P_1}{\left(2mr^2T\right)^{1/2}} \right) \right.$$

$$\left. - \mathrm{erf} \left(\frac{mr^2\omega/2 - P_1}{\left(2mr^2T\right)^{1/2}} \right) \right]$$

For large argument, we have

$$\frac{1}{2} e^{\phi/T} \mathrm{erfc} \left(\frac{mr^2\omega/2 - P_1}{\left(2mr^2T\right)^{1/2}} \right)$$

$$= \frac{1}{2\sqrt{\pi}} \left(\frac{\left(2mr^2T\right)^{1/2}}{mr^2\omega/2 - P_1} \right)$$

$$\times \exp \left[- \frac{P_{min} - P_1}{\left(2mr^2T\right)^{1/2}} \left| \frac{P_{min} - P_1}{\left(2mr^2T\right)^{1/2}} + 2 \left(\frac{e\phi}{T} \right)^{1/2} \right) \right]$$

and similarly for P_2 .

Other Cases:

Other cases may be derived from these, if we add P_1, P_2 as arguments to ρ_A, ρ_B, ρ_C.

$$\frac{\rho_A}{\rho} = F_A \left(r, \phi, P_1, P_2 \right) , \text{ etc.}$$

We then have,

Case D: $\quad P_2 > P_{max} > P_1 > mr^2\omega/2 \left[1 - \left[\dfrac{8e\phi}{mr^2_r 2} \right]^{1/2} \right]$

$$\frac{\rho_D}{\rho} = F_A \left(r, \phi, P_{max}, P_2 \right) + F_B \left(r, \phi, P_1, P_{max} \right) \quad .$$

Case E: $\quad P_2 > P_{max} > P_{min} > P_1$

$$\frac{\rho_E}{\rho} = F_A \left(r, \phi, P_{max}, P_2 \right) + F_B \left(r, \phi, P_{min}, P_{max} \right) + F_C \left(r, \phi, P_1, P_{min} \right)$$

Case F: $\quad P_{max} > P_2 > P_{min} > P_1$

$$\frac{\rho_F}{\rho} = F_B \left(r, \phi, P_{min}, P_2 \right) + F_C \left(r, \phi, P_1, P_{min} \right)$$

33